

# QUALITY ASSESSMENT OF THE VITREOUS ENAMEL COATING APPLIED TO THE WELD JOINT

KRISTYNA STERNADELOVA<sup>1</sup>, HANA KRUPOVA<sup>1</sup>, DALIBOR MATYSEK<sup>2</sup>, PETR MOHYLA<sup>1</sup>

<sup>1</sup>VSB – Technical University of Ostrava, Faculty of Mechanical Engineering, Ostrava, Czech Republic

<sup>2</sup>VSB – Technical University of Ostrava, Faculty of Mining and Geology, Ostrava, Czech Republic

DOI: 10.17973/MMSJ.2023\_03\_2022105

kristyna.sternadelova@vsb.cz

This work compares different thicknesses of vitreous enamel coating applied to welded joints. Low-carbon steel Kosmalt E300T was used as a base material. The MAG welding method was used for all samples. Metallography was performed to compare the thickness of the coating formed on the machined and unmachined surfaces of the weld. SEM analysis focused on the substrate/vitreous enamel coating interface. The results show that the high thickness of the vitreous enamel coating that occurs in unmachined weld joints significantly decreases the properties of the enamel coating. In comparison, the machining of the weld surface contributes to the quality improvement of the vitreous enamel coating.

## KEYWORDS

Vitreous Enamel, Enamel Coating, Welded Joints, Enamel Interface, Surface Treatment.

## 1 INTRODUCTION

The most commonly used material in industry is steel. Despite its good mechanical properties [Maziarz 2022, Pastrnak 2021, Szkandera 2021, Mohyla 2014, Rusz 2019], it needs to be protected from degradation by surface treatment due to its high reactivity with the environment. Crucial moment before any surface treatment is correct pretreatment [Cada 2021] that goes hand in hand with proper material treatment during production [Cada 1997, Cada 2003, Novak 2019]. In the case of the welding the mechanical properties of the material are important, especially in the heat-affected zone [Sternadelova 2019, Mohyla 2014]. Weld technology affects the deformation properties of steels [Evin 2016] as well as the resistance to corrosion.

In the manufacturing process, a properly designed maintenance organisation [Necas 2019, Necas 2021, Schindlerova 2021] and the monitoring and prevention of defects [Sproch 2021] are also important. The achievement of maximum production productivity while eliminating waste can be achieved, for example, by using the Value Stream Mapping Method [Sajdlerova 2015, Schindlerova 2019].

Enamel coatings are often used in industry due to their corrosion resistance; resistance to mechanical wear, high temperatures and chemicals [Bouse 1986]. In turn, their aesthetic appearance and ease of cleaning can be exploited in certain applications [Podjuklova 2010].

The functionality of the resulting coating is influenced by the strong network of bonds between the base metal and the amorphous glassy coating formed during the firing of the applied enamel slurry. This interface is one of the most critical aspects affecting the properties and quality of the enamel coating.

The mechanism of the metal/enamel interface has been studied in the past [Mohyla 1990, Zucchelli 2012], but due to its complexity this issue requires further research using new technologies.

Previous research [Sternadelova 2021] shows that the thickness of the coating has a non-negligible effect on the resulting quality of the enamel coating. When enamelling weld joints, enamel slurry may accumulate in the vicinity of the weld before firing, leading to greater thickness in the surroundings of the weld. In the present work, we focus on comparing the effect of weld joint machining on the resulting enamel coating thickness. The accumulation of enamel slurry during application in the vicinity of surface macro-roughness leads to a local increase in coating thickness, which in turn leads to a reduction in mechanical properties. By removing the macro-roughness (weld joint alignment by grinding), we expect this phenomenon (commented on in previous research) to be reversed. At the same time, we anticipate that analysis of the specimen surface by electron microscopy will help to bring understanding into the mechanism of the formation of the base material/enamel interface.

## 2 EXPERIMENTAL

### 2.1 Base material

Low carbon steel Kosmalt E 300 T was used as a base material in this work according to our previous work [Sternadelova 2021]. The composition of the base material was analyzed by GDOES method, and the results are shown in Table 1.

Element	Base metal	Weld Metal
C	0.039	0.064
Mn	0.195	0.942
Si	0.027	0.605
P	0.013	0.011
S	0.011	0.014
Al	0.048	0.009
Cu	0.021	0.026
Ti	0.060	0.007

Table 1. Composition of the base metal and weld metal in Wt. %

### 2.2 Sample preparation

In total, 4 groups of specimens were prepared, differing in surface pretreatment and weld surface processing. From all the prepared samples, 4 samples representing each group (R-2.1A, R-2.2B, RB-2.3A, RB-2.4B) were then selected for further analysis. The samples are 198 x 90 mm in size and 5 mm thick. The samples marked as RB-2.3A, RB-2.4B have a grinded surface of the weld.

All samples were welded by ABB IRB 1660 ID-4 welding robot by the method 135 (MIG/MAG) with solid wire OK AristoRod 12.50 (C=0.10 %, Mn=1.50 %, Si = 0.90 %, ESAB). The weld gap ranged from 1.0 to 1.6 mm. The welding current ranged from 210-250 A and the voltage ranged from 18-24 V. Shielding gas M21 (82 % Ar + 18 % CO<sub>2</sub>) was used with the flow rate of 12 l/min, welding speed of 5 mm/s was applied.

### 2.3 Pretreatment

Pickling was used as a distinguishing parameter of pretreatment for a set of A samples (R-2.1A, RB-2.3A). First, they were degreased in Simple Green industrial degreasing agent in ratio 1:15 with distilled water at room temperature for 20 minutes followed by a rinse with distilled water. Then, the samples were pickled in 10 % HCl solution at 27 °C for 18 minutes followed by a rinse with distilled water. After the pickling process, neutralisation is an essential step in the pretreatment procedure. It was carried out in 10 % NaOH solution at 40 °C for

4 minutes. After neutralisation, the samples were rinsed with distilled water and then dried in an oven at 100 °C.

For another group of samples, set of B samples (R-2.2B, RB-2.4B), surface pickling was replaced by blasting. First, the samples were degreased in an aqueous solution of Simple Green industrial degreaser (mixed 1:15 with distilled water) at room temperature for 20 minutes followed by a rinse with distilled water. Then the surface of the samples was treated by blasting with silica sand as a blasting material. Finally, the samples were rinsed with distilled water and dried in a drying oven at 100 °C.

## 2.4 Enameling

Base enamel frit was purchased from Ferro and cover enamel frit was purchased from Mefrit. Both layers of base and cover enamel were applied by hand spraying with pressure gun. First, the base enamel layer was applied, dried and then fired at 840 °C for 12 minutes. After cooling, the cover enamel layer was applied, dried and then fired in muffle furnace LAC L15/12 at 30 °C for 9 minutes.

## 3 RESULTS

### 3.1 Thickness measurement

Thickness measurement of both enamel layers was performed in three separate areas, using Elcometer 456 digital thickness gauge, in accordance with EN ISO 2178 standard. Thickness was measured above the weld (Area 1), on the weld area (Area 2) and below the weld (Area 3). For a better illustration, the locations over which the thickness was measured are shown in Figure 1. The data obtained from the measurement are summarized in Table 2.



Figure 1. Measured areas

Sample	Area 1		Area 2		Area 3	
	Mean	Std.Dev.	Mean	Std.Dev.	Mean	Std.Dev.
R-2.1A	510.0	14.43	616.0	7.87	506.6	10.99
R-2.2B	382.3	6.31	439.4	9.00	483.9	10.08
RB-2.3A	496.0	8.01	492.8	24.45	447.4	15.92
RB-2.4B	467.4	8.25	439.0	16.63	387.7	7.83

Table 2. Coating thickness - measured mean values in  $\mu\text{m}$

For better visualisation of the results, we opted for a graphical display that shows the comparison of each area for each sample and gives better understanding of the effect of mechanical machining of the weld joint before subsequent surface treatment. The graphical illustration is included in Figure 2.

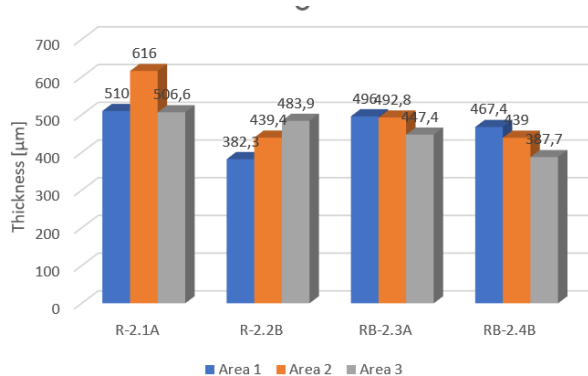


Figure 2. Coating thickness measurement - mean values

### 3.2 Microhardness measurement

The measured properties of the enamel coating include its microhardness. Microhardness was measured in accordance with EN ISO 4516 standard using the microhardness testing machine LECO LM247AT. The measurements were performed using the Knoop method with load of 100 g. The measurement results for all samples are shown in Table 3.

Sample	Base layer		Cover layer	
	Mean	Std.Dev.	Mean	Std.Dev.
R-2.1A	550	18.65	535	43.95
R-2.2B	539	33.56	555	68.42
RB-2.3A	597	63.78	513	58.02
RB-2.4B	543	50.00	592	51.66

Table 3. Measured microhardness values,  $\text{HK}_{0,1}$

### 3.3 Metallographic analysis

The metallographic analysis of the specimen reveals what the vitreous enamel coating looks like on the cross-section. If there are defects in the coating, how big they are or what is their distribution in the coating. If the coating consists of multiple layers, as in our case, we can also visually compare the defects in the enamel layers in the cross-section. Measuring the thickness by a non-destructive method only gives us the overall thickness of the enamel coating. Therefore, the thickness was also measured on a microstructure cross-section of the enamel coating. In the following, there is presented detailed microstructure (Figure 3, Figure 5, Figure 7, Figure 9) and macrostructure (Figure 4, Figure 6, Figure 8, Figure 10) of the cross-section of all analysed samples. The microstructure images show that the cover layer contains, compared to the base layer of the enamel coating, large, closed pores that are embedded in the structure of the coating.

Based on the carried experiments, the influence of the thickness of the vitreous enamel coating on its mechanical properties can be observed. In the case of samples (group RB) with machined weld surface, no chipping of the vitreous enamel coating occurred during sample preparation (cutting) for metallographic analysis. In the second group of samples (group R), the large thickness of the coating around the welded joint led to the previously mentioned chipping of the vitreous enamel coating.

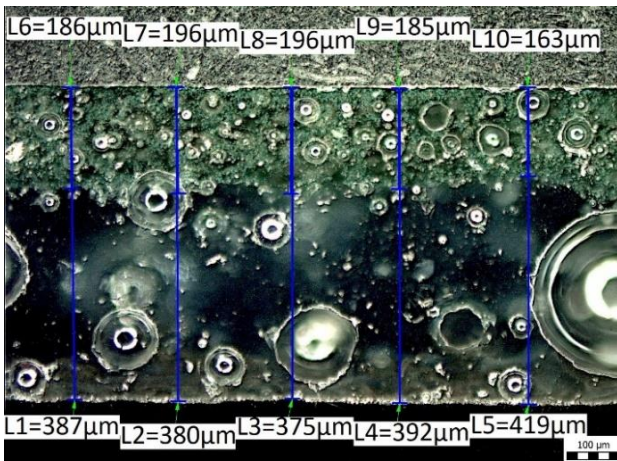


Figure 3. Microstructure of the sample R-2.1A, cover layer situated on the bottom

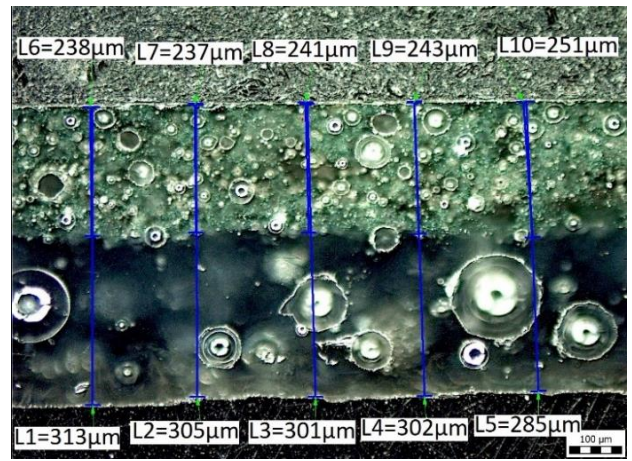


Figure 7. Microstructure of the sample RB-2.3A



Figure 4. Macrostructure of the sample R-2.1A, the scale in the bottom right corner represents 2 mm

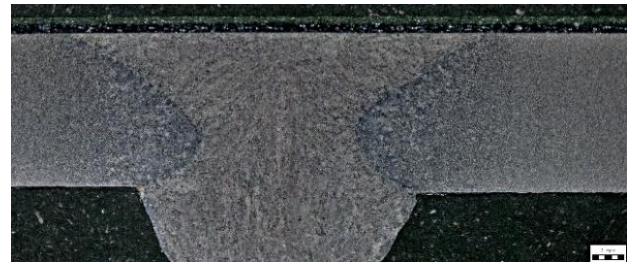


Figure 8. Macrostructure of the sample RB-2.3A, the scale in the bottom right corner represents 2 mm

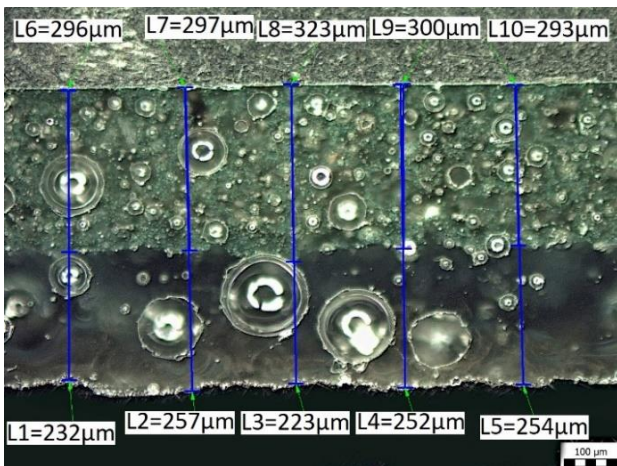


Figure 5. Microstructure of the sample R-2.2B

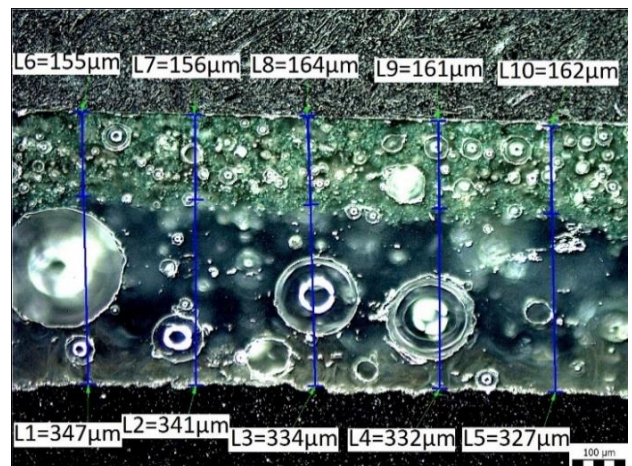


Figure 9. Microstructure of the sample RB-2.4B



Figure 6. Macrostructure of the sample R-2.2B, the scale in the bottom right corner represents 2 mm



Figure 10. Macrostructure of the sample RB-2.4B, the scale in the bottom right corner represents 2 mm

### 3.4 SEM analysis

As mentioned in the introduction, today's imaging methods can help us to specify more precisely what structures are contained in the base material/vitreous enamel interface. Chemical composition analysis, based on the energy levels of the detected electrons reflected from the sample, determines what the chemical composition of these structures are at the analysed location of the sample. Therefore, we etched the enamel coating and then analysed the surface on a scanning electron microscope. A detailed image of the surface revealed the presence of iron and silicon-based structures [Mohyla 1990].

On a scanning electron microscope FEI Quanta 650 FEG (TermaFisher Scientific), we observed sample RB-2.4B, a sample that had been blasted with silica sand prior the application of the enamel coating. The sample was etched in an aqueous solution of HF (in ratio 1:3 with distilled water) for 3 hours. The measurements were performed in backscattered electron detection mode at an accelerating voltage of 20 keV. On visual inspection of the specimen, the vitreous enamel coating was etched away to the base metal in some areas. In other places we observed remnants of vitreous enamel coating (defined by darker colour than base metal). Detailed image of the sample surface is situated in Figure 11. According to the energy dispersion x-ray spectra (EDX) the darker spots correspond to residues of enamel coating. An example of the EDX of the lighter spot is shown in Figure 12. According to the chemical composition it can be concluded that these are structures formed by the combination of base metal and enamel coating.

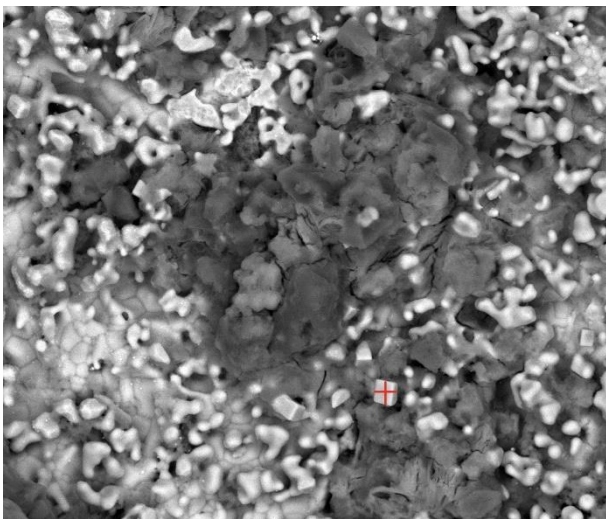


Figure 11. SEM image (3891x magnification) of the RB-2.4B sample surface with marked spot for EDX analysis

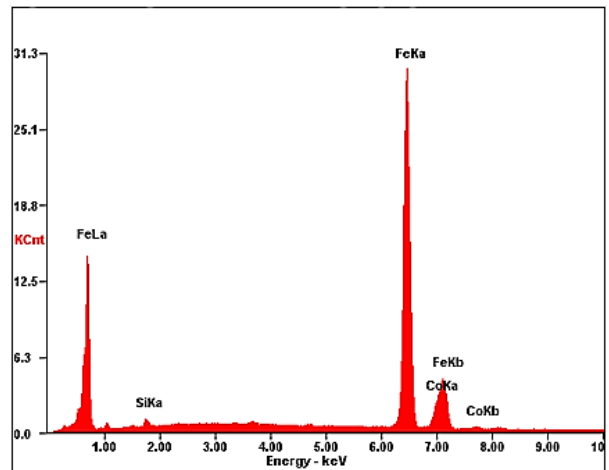


Figure 12. EDX spectra for a specific point on the RB-2.4B sample surface.

Figure 13 contains an enlarged crystalline structure we found on the RB-2.4B sample surface. Further EDX analysis (Figure 14) shown that this structure chemically consists of iron and oxygen. It can be the compound, which forms the metal/enamel interface.

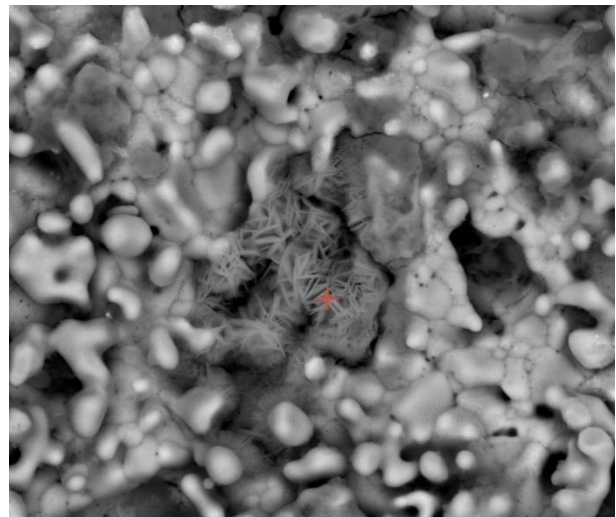


Figure 13. SEM image (8000x magnification) of the RB-2.4B sample surface with marked spot for EDX analysis

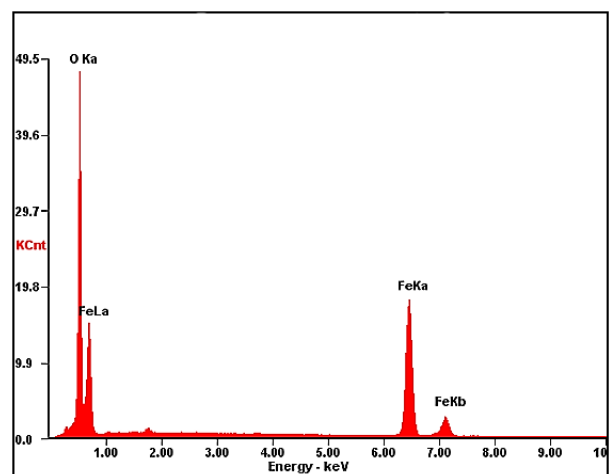


Figure 14. EDX spectra for a specific point on the RB-2.4B sample surface

## 4 CONCLUSIONS

The aim of the work was to evaluate the effect of weld joint machining on the resulting thickness of the enamel coating. Different types of pretreatment - pickling and blasting - were used. From previous research [Sternadelova 2021] is obvious that manual application of enamel slurry results in its accumulation near the weld. The top of the weld bead is covered with a coating of lower thicknesses due to gravitational forces and surface tension. Higher coating thickness negatively affects the properties of the vitreous enamel coating. If the weld is grinded prior to the application of the enamel slurry, no enamel slurry builds up during the application and therefore the thickness of the enamel coating is uniform also in the surroundings of the weld. The work showed that large deviations in coating thickness led to chipping under mechanical loading of the coating. Therefore, uniformity of thickness provides better mechanical properties of the coating. The coating layers are also less prone to damage thus provide better protection of the base material.

At the same time, advanced imaging methods were used to analyse the surface of the base material after the enameling process. The chemical composition (obtained by EDX analysis) of the compounds situated just in the base metal/vitreous enamel coating boundary was evaluated.

## ACKNOWLEDGMENTS

The research was supported by SP2022/14 specific research project "Research and Development of Engineering Technologies and their Management".

## REFERENCES

- [Bouse 1986] BOUSE, V. et al. *Enamels and their Use in Corrosion Protection*. Prague: Technical Literature Publishing House, 1986. (in Czech)
- [Cada 1997] CADA, R. Formability of Deep-Drawing Steel Sheets. In: *Materials, Functionality & Design, Proceedings of the 5th European Conference on Advanced Materials and Processes and Applications EUROMAT 97*. Maastricht, The Netherlands, 1997, pp. 463-466, ISBN 90-803513-4-2.
- [Cada 2003] CADA, R. Testing of Strain in Stampings by Embossed Grids. *Technical Gazette*, 2003, Vol. 10, No. 3-4, pp. 9-13. ISSN 1330-3651.
- [Cada 2021] CADA, R. and LOSAK, P. Optimization of Bellows and Tubes Cutting by Disc Knife to Achieve the Minimum Burr Size. *Modern Machinery (MM) Science Journal*, 2021, Vol. 14, No. 6, pp. 5373-5380. ISSN 1803-1269, eISSN 1805-0476.
- [Evin 2016] EVIN, E. et al. Laser-Beam Welding Impact on the Deformation Properties of Stainless Steels when Used for Automotive Applications. *Acta Mechanica Automatica*, 2016, Vol. 10, No. 3, pp. 189-194. ISSN 1898-4088.
- [Maziarz 2022] MAZIARZ, W. et al. Effect of Severe Plastic Deformation Process on Microstructure and Mechanical Properties of AlSi/SiC Composite. *Journal of Materials Research and Technology*, 2022, Vol. 17, pp. 948-960. ISSN 2238-7854 (Online).
- [Mohyla 1990] MOHYLA, M. et al. A Contribution to the Study of the Phase Boundary Between Metal and Vitreous Enamel. *CERAMICS*, 1990, Vol. 34, No. 4, pp. 299-304.
- [Mohyla 2014] Mohyla P. et al. Evaluation of Creep Properties of Steel P92 and Its Welded Joint. *METALURGIJA*, 2014, Vol. 53, No. 2, pp. 175-178.
- [Necas 2019] NECAS, L. Training and Practice to Ensure Implementation of the TPM System. *Modern Machinery (MM) Science Journal*, 2019, Vol. 12, No. 2 (June), pp. 4124-4127. ISSN 1803-1269, eISSN 1805-0476.
- [Necas 2021] NECAS, L. and NOVAK, J. Networking of Maintenance Entities for Production and Other Processes. *Modern Machinery (MM) Science Journal*. 2021, Vol. 14, No. 6, pp. 5410-5413. ISSN 1803-1269, eISSN 1805-0476.
- [Novak 2019] NOVAK, V. et al. The Effect of Strain Rate on Position of Forming Limit Curve. In: *28th International Conference on Metallurgy and Materials (Metal 2019)*. Ostrava, Czech Republic: TANGER, Ltd. 2018, pp. 378-383.
- [Pastrnak 2021] PASTRNAK, M. et al. Effect of Processing Route on Microstructure and Microhardness of Low-Carbon Steel Subjected to DRECE Proces. In: *30th International Conference on Metallurgy and Materials (METAL 2021)*. Ostrava, Czech Republic: TANGER, Ltd., 2021, pp. 323-328. ISBN 978-80-87294-99-4. ISSN 2694-9296 (Online).
- [Podjuklova 2010] PODJUKLOVA, J. et al. *New Horizons in the Knowledge of the Properties of Glass-Ceramic Enamel Coatings*. Ostrava: VSB – Technical University of Ostrava, 2010. ISBN 978-80-248-2339-3.
- [Rusz 2019] RUSZ, S. et al. Influence of SPD Process on Low-Carbon Steel Mechanical Properties. *Modern Machinery (MM) Science Journal*, 2019, Vol. 12, No. 2, pp. 2910-2914. ISSN 1803-1269 (Print), ISSN 1805-0476 (On-line).
- [Sajdlrova 2015] SAJDLEROVA, I. et al. Potential of Value Stream Mapping Utilization in the Seamless Steel Tubes Manufacturing Process. In: *24th International Conference on Metallurgy and Materials (Metal 2015)*. Ostrava, Czech Republic: TANGER, Ltd., 2015, pp. 2056-2064. ISBN 978-80-8729462-8.
- [Schindlerova 2019] SCHINDLEROVA, V. et al. Potential of Using Simulation for the Design of Distribution Warehouse. In: *8th Carpathian Logistics Congress on Logistics, Distribution, Transport and Management (CLC)*. Prague, Czech Republic: TANGER, 2019, pp. 802-807.
- [Schindlerova 2021] SCHINDLEROVA, V. and SAJDLEROVA, I. Comparison of Basic Maintenance Concepts Using Witness. *Modern Machinery (MM) Science Journal*. 2021, Vol. 14, No. 6, pp. 5435-5440. ISSN 1803-1269, eISSN 1805-0476.
- [Sproch 2021] SPROCH, F. and NEVIMA, J. Use of Smart 3D Printing Technology in Conventional Engineering Production to Detect and Prevent the Occurrence of Defects. *Modern Machinery (MM) Science Journal*. 2021, Vol. 14, No. 6, pp. 5441-5447. ISSN 1803-1269, eISSN 1805-0476.
- [Sternadelova 2019] STERNADELOVA, K. et al. Properties and Microstructure of Modeled Heat-Affected Zone of P92 Steel. In: *28th International Conference on Metallurgy and Materials (Metal 2019)*. Ostrava, Czech Republic: TANGER, 2019, pp. 832-836. ISBN 978-80-87294-92-5. ISSN 2694-9296.
- [Sternadelova 2021] STERNADELOVA, K. et al. Problems with Surface Protection of Welded Joints by Vitreous Enamel Coating. In: *6th International Conference on Recent Trends in Structural Materials (COMAT 2020) IOP Conference Series: Materials Science and Engineering*. Pilsen, Czech Republic, 2021, p. 1178.
- [Szkandera 2021] SZKANDERA, P. et al. Influence of DRECE Method on Mechanical Properties of Different Low Carbon Steel. In: *30th International Conference on Metallurgy and Materials (METAL 2021)*. Ostrava, Czech Republic: TANGER, Ltd., 2021, pp. 211-216. ISBN 978-80-87294-99-4. ISSN 2694-9296 (Online).

[Zucchelli 2012] ZUCCHELLI, A. et al. Characterization of Vitreous Enamel-Steel Interface by Using Hot Stage ESEM and Nanoindentation Techniques. *Journal of the European Ceramic Society*, 2012, Vol. 32, No. 30, pp. 2243-2251.

**CONTACTS:**

Kristyna Sternadelova, MSc

VSB – Technical University of Ostrava, Faculty of Mechanical Engineering, Department of Mechanical Technology  
17. listopadu 2172/15, 708 00 Ostrava-Poruba, Czech Republic  
+420 596 993 721, [kristyna.sternadelova@vsb.cz](mailto:kristyna.sternadelova@vsb.cz), [www.fs.vsb.cz](http://www.fs.vsb.cz)

Hana Krupova, MSc

VSB – Technical University of Ostrava, Faculty of Mechanical Engineering, Department of Mechanical Technology  
17. listopadu 2172/15, 708 00 Ostrava-Poruba, Czech Republic  
+420 596 993 524, [hana.krupova@vsb.cz](mailto:hana.krupova@vsb.cz), [www.fs.vsb.cz](http://www.fs.vsb.cz)

Dalibor Matysek, Dr.

VSB – Technical University of Ostrava, Faculty of Mining and Geology, Department of Geological Engineering  
17. listopadu 2172/15, 708 00 Ostrava-Poruba, Czech Republic  
+420 596 994 540, [dalibor.matysek@vsb.cz](mailto:dalibor.matysek@vsb.cz), [www.hgf.vsb.cz](http://www.hgf.vsb.cz)

Petr Mohyla, prof.

VSB – Technical University of Ostrava, Faculty of Mechanical Engineering, Department of Mechanical Technology  
17. listopadu 2172/15, 708 00 Ostrava-Poruba, Czech Republic  
+420 596 993 115, [petr.mohyla@vsb.cz](mailto:petr.mohyla@vsb.cz), [www.fs.vsb.cz](http://www.fs.vsb.cz)